

3D Numerical Simulation of Micro-Jet Excitation

Luka S. Volkov¹ , Aleksandr A. Firsov¹ 

© The Authors 2025. This paper is published with open access at SuperFri.org

Excitation of round laminar air micro-jet by volumetric force and by pulse-periodic heat source was simulated using the FlowVision software package in 3D formulation at normal conditions. Heat source and volumetric force imitate an influence of electrical discharge. Air jet was formed by a circular cross-section channel with inner size of 1 mm with the Poiseuille velocity profile at inlet boundary, the maximum profile velocity was 5 m/s. The conditions corresponded to the formulation of the problem considered earlier in the experiment. Dependence of large-scale vortex formation from volumetric force frequency and amplitude was obtained. Amplitude of force corresponding to the effect of the discharge on the air jet was determined and was set to 5 μN . For round laminar jet the excited oscillations of the jet was obtained at frequency range 500–2500 Hz, further increase in the frequency of oscillations left the shape of the jet close to the initial. Lack of influence of pulse-periodic heat source on flow structure was discussed. The results obtained demonstrate that the main contribution from the corona discharge to the jet in the experiment is provided by the volumetric force (ionic wind), and not by the heating of the gas.

Keywords: micro-jet, excitation, discharge, instability, numerical simulation.

Introduction

Studies of the stability of laminar jet flows and the mechanisms of their instability and excitation are of significant interest for various applications, including burners and combustion chambers of various types, chemical reactors, and medical devices [1]. For example, micro-jets are used to control the flow pattern and structure of a large diameter jet [2]. A significant part of investigations is dedicated to the so-called micro-jets with a diameter of no more than 1 mm, the excitation of which by volumetric force and heat source will be investigated in this work. The flow in micro-jets differs significantly from macrojets, the conditions for vortex formation change, and the penetration depth increases [3]. Similar studies of the stability of micro-jets are carried out not only in gases, but also in liquids; thus, in work [4] the transition of a laminar jet to newtonian turbulence, elasto-inertial filaments, and elasto-inertial turbulence is described, depending on the addition of polymer.

The velocity profile in the nozzle influences the position of laminar-turbulent transition and/or excitation of various types of instabilities. The closer the profile is to the Poiseuille (parabolic), the further from the nozzle the transition and/or excitation of various types of instabilities occurs. The parabolic profile forms due to the growth of the boundary layer. Therefore, to obtain extended laminar jets, the diameter d of the gas channel should be much smaller than its length L ($L/d > 100$). In the practical applications [5, 6] both the stabilization of laminar jets and the early excitation of instabilities are of interest. The excitation leads to increased jet mixing with the surrounding gas (moving or stationary) and intensification of combustion.

The classical method of jet excitation is to use acoustic vibrations [7]; however, in most works the use of a plane wave is discussed, i.e., non-local influence [8–10]. Thus, in [11] the bifurcation of a propane micro-jet under external acoustic influence and an increase in flame stability are shown. In addition to the excitation of instability or bifurcation of the jet, acoustic radiation contributes to reducing NO_x concentration during the combustion of a laminar hydrogen jet in

¹Joint Institute for High Temperatures of the Russian Academy of Sciences (JIHT RAS), 125412, Moscow, Russia

the air [12]. However, in recent works the local acoustic influence is also considered – but it is discussed in relation to turbulent jets, for example, in [13, 14] the excitation of a turbulent jet is investigated using local input of acoustic radiation at the nozzle edge.

Electrical discharges of various types can provide local effects: form shock waves, be a source of volumetric force and heat generation. For example, spark discharges have been considered in various settings as an actuator that intensifies the mixing of a transverse gas jet with a supersonic air flow, both experimentally [15] and using numerical modeling [16, 17]. In [18], the possibility of excitation and turbulence of a laminar jet using a corona discharge was experimentally investigated; bifurcation of the jet with a rapid transition to turbulence was shown by analogy with works on acoustic excitation [11]. Analysis of the literature showed that it is noteworthy that the stability of micro-jets and the possibility of their excitation using acoustic vibrations through numerical modeling were practically not considered, with rare exceptions [19] where the instability of a plane (two-dimensional) jet was considered. At the same time, such works are known for turbulent jets, for example, in work [20] the instability and bifurcation of a turbulent jet caused by a pulsed micro-jet impact located on the nozzle edge were considered using DNS modeling. In our previous work, the fundamental possibility of modeling the excitation of a flat (two-dimensional) microjet using an acoustic impact or a heat source in FlowVision was considered, and positive results were obtained [21]. FlowVision is a commercial heavy industrial CFD code that is used both for fundamental research and for solving applied problems [22, 23]. Therefore, it looks relevant to consider, using 3D numerical modeling by FlowVision, the stability of the round laminar microjet and the possibility of its local excitation using a pulse-periodic force or energy input simulating a corona discharge under the conditions corresponding to experimental research [18].

The article is organized as follows. Section 1 is devoted to description of a simulation model and boundary conditions. In Section 2 we discuss the amplitude of volumetric force at which the results obtained in the simulation will coincide well with the experiment on the effect of a corona discharge on an air jet. Section 3 represents the results of the simulation for fixed jet velocity 5 m/s at varying the frequency of the discharge. And Section 4 demonstrates the lack of influence of pulse-periodic heat source on flow structure. Conclusion summarizes the study and reveals that the main contribution from the corona discharge to the jet in the experiment is provided by the volumetric force (ionic wind), and not by the heating of the gas.

1. Model and Boundary Conditions

Obtaining detailed information on the distribution of gas-dynamic quantities is significantly difficult in an experiment on excitation of a laminar micro-jet using an electric discharge. Numerical modeling can be used to obtain information about pressure and velocity fields throughout the volume of interest. Previous attempt to describe the influence of discharge by numerical simulation was performed in a 2D formulation [21] to evaluate the capabilities of the software and due to limited computing resources. Having a license of FlowVision for computing on 64 cores and a PC based on AMD Ryzen 9 3900X (12 cores), equipped with 64 GB of memory, as well as the possibility to use the nodes of the “Fischer” supercomputer of JIHT RAS based on AMD Epyc 7301 / AMD Epyc 7551 (16 / 32 cores), it was decided to perform three-dimensional modeling of the excitation of a circular laminar air jet by discharge.

Numerical modeling of the excitation of a jet by the operation of a discharge was performed using the FlowVision 3.14 software package. The simulation is based on solving a three-

dimensional unsteady system of Navier–Stokes equations with second-order central difference scheme of accuracy. The turbulence model was disabled, and taking into account fairly large cell size and schematic viscosity, the simulation performed is closer to LES than to DNS.

The calculation area is a cylinder with a length (along the stream) of 60 mm and a diameter of 50 mm and is presented in Fig. 1. There is a tube 5 mm long with an internal diameter of 1 mm and an external diameter of 1.2 mm located along the x-axis on one of the boundaries. At the distance of 3 mm from the edge of the tube there is an area of volumetric force or volumetric heat, simulating the operation of a discharge. The project used a rectangular computational mesh (Fig. 2) with adaptation: an increased level of adaptation (refinement of the computational mesh) was used in the area of air jet flow. The cells near the boundary conditions have a complex shape because they are cut off by geometry. Thus, inside the tube there are 46 cells per channel diameter, and the total number of cells in the project did not exceed 5 million. The simulation required the use of a small time step ($CFL < 1$) and it was set to $2 \mu s$.

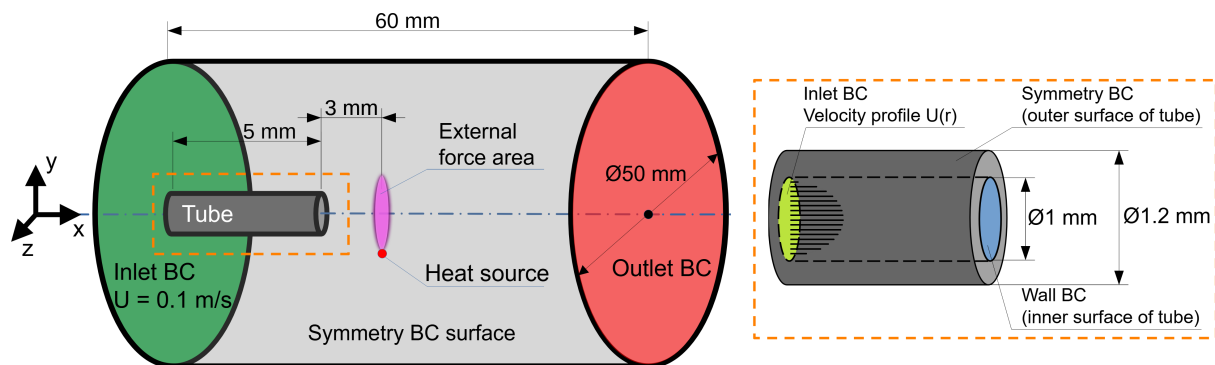


Figure 1. Calculation domain and boundary conditions

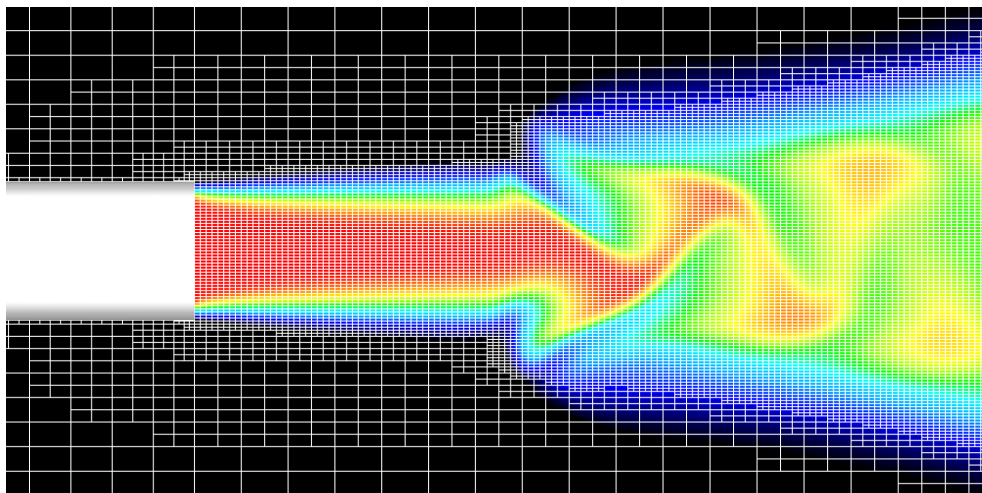


Figure 2. Computational grid on the background of jet passive scalar

The “wall” boundary condition (no-slip boundary) was used on the inner wall of the tube and on the edge; a Poiseuille velocity profile was installed at the entrance of the tube; the maximum profile speed U_0 was set to 5.0 m/s. At the entrance to the computational domain from the side of the tube, a constant velocity boundary condition of 0.1 m/s was set to minimize the mutual influence of pulsations created by the discharge. The working gas was air. In all

calculations, to accurately determine the jet passive scalar, two identical substances were used, both having the properties of air: “Air1” as jet and “Air2” as ambient medium. Jet passive scalar is then defined as $Y = [Air1]/([Air1] + [Air2])$, where $[X]$ is mass concentration of X . This made it possible to visualize the jet similarly to visualization using smoke/spray in the experiment.

On the outer walls of the tube, as well as along the curved surface of the cylindrical computational domain, a symmetry condition was established (a surface with flow slip and zero gradient of all values). At the remaining boundary opposite the tube, zero relative total pressure was established (i.e., the total pressure was equal to the reference pressure). The relative temperature at all permeable boundaries was set to zero. The reference temperature and pressure were set to 273 K and 101000 Pa, respectively. Thus, the simulation parameters corresponded closely to the setup described in the experimental work [18].

2. Choosing the Amplitude of Volumetric Force

It is well known that a corona discharge causes an ion wind (a directed gas jet) and is also a weak source of heat. To simulate the effect of a corona discharge on a laminar jet by volumetric oscillating force, it is necessary to know the amplitude of the force. For example, in the work [24], the volumetric force characteristic of a dielectric barrier discharge is indicated as a 2–5 μN and the corona discharge is close to it in type [25]. In accordance with these data, the amplitude of the integral force was tested in the range of 1–10 μN . The external force was applied to an elliptical shape region marked in Fig. 1, the chosen shape of the volume force region approximately corresponds to the effect observed in the experiments [24, 25].

In this paper, the dependence of force on time is assumed as sinusoidal. However, it should be noted that this is a simplification. Due to the peculiarities of the corona discharge, in reality the force acting on the jet is expected to depend on time in a more complex way. Nevertheless, in this study, it was decided to limit ourselves to the effect of a sinusoidal external force, i.e., corresponding to a narrow spectrum in Fourier space.

The data from [18] were used as a basis for determining the amplitude of the external force: the photographs of a seeded laminar jet excited by a corona discharge. In [18], photographs of the jet are given for several values of the amplitude of the voltage in the discharge at a fixed frequency of 1500 Hz, but data on the volumetric force are missing. For several values of the voltage in the simulation, the corresponding amplitude of the external sinusoidal force was selected.

The comparison of the experiment and the simulation was carried out as follows. The divergence angle of the jet streams was measured. According to the experimental images, this angle was determined by a clearly visible boundary between the dark and seeded areas. In the simulation, straight lines were drawn through areas with a given value of the passive scalar (substance fraction) of the jet to determine the angle. By comparing the divergence angle in the simulation and in the experiment, the corresponding values of the external force amplitude in the simulation were selected for several values of the discharge voltage. Figure 3 shows the photographs of the jet from the article [18] and the results of the computer simulation in a single scale.

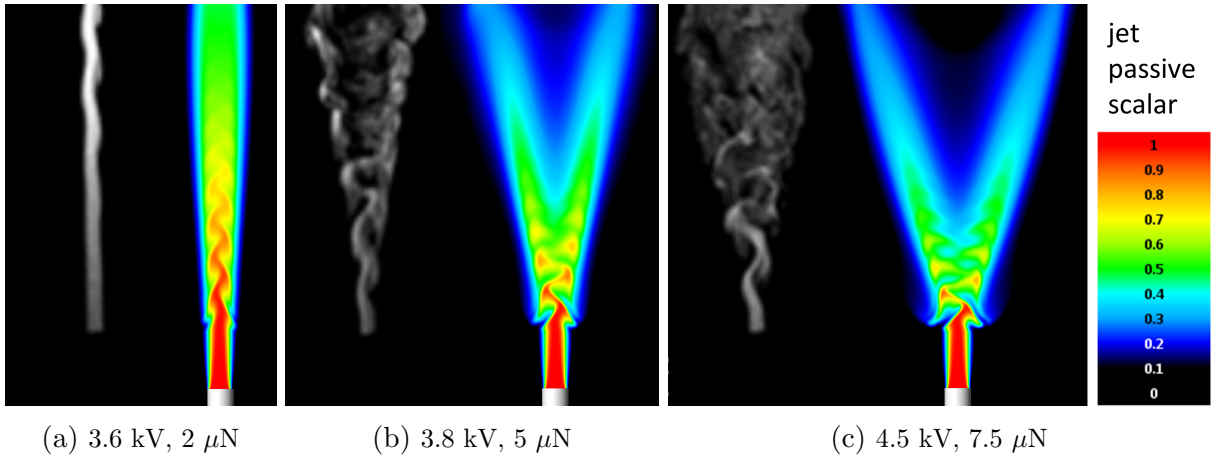


Figure 3. Comparison of experiment (with different crown discharge voltage) and simulations (with different force amplitude). The experiment is shown in grayscale (spray visualization) and the simulation is shown as a color scale

3. Results for Fixed Jet Velocity at Varying the Frequency of the Discharge

In this part of the research, the amplitude of the force $F = 5 \mu N$ was selected. It corresponds to the amplitude of the voltage in the discharge of 3.8 kV, because at this voltage the dependence of the flow configuration on frequency was studied in the experiment. The jet was modeled under the action of a periodic external force with a frequency of 500 to 2500 Hz. The goal of this part of the work was a qualitative observation of the jet response to action with different frequencies. A comparison of the obtained distributions of the passive scalar of the jet with the images from the article [18] for several frequencies is shown in Fig. 4.

At the highest frequency of 2500 Hz, visible oscillations similar to those observed in the experiment are formed in the jet. But the jet in the simulated section has only one stream, i.e., in each cross-section of the jet there is only one local maximum of the jet passive scalar.

At lower frequencies (this is especially pronounced for 1500 Hz), the jet splits into two streams in the plane formed by the initial velocity vector and external force vector. The jet splitting point is arbitrary, since the passive scalar on the jet axis decreases smoothly. However, this qualitative transition occurs closer to the injector in cases with lower frequencies.

For a frequency of 1000 Hz, a significant discrepancy between the simulation and experimental results begins. This can be explained by the fact that in reality a time dependence of the force differs from the sinusoidal one, and at low frequencies this difference is most pronounced. At a low frequency of the external force, 500 Hz, the jet does not just break up into two branches, but splits into separate fragments drifting along the flow.

Next, the structure of the jet is studied in detail using the example of one particular case (1500 Hz, $5 \mu N$), and the processes that determine the mixing of the jet with the external flow are analyzed. Figure 5 shows a three-dimensional visualization of the jet structure for the case of 1500 Hz. The lines on two planes mark the position of the jet boundary, drawn at the level of 50% of the jet passive scalar. The ellipsoid marks a position of the area with a volumetric force. The force vector is parallel to y-axis. The jet has almost no oscillations in the direction perpendicular to the force vector. The disturbances caused by the external force are most pronounced in the x-y plane.

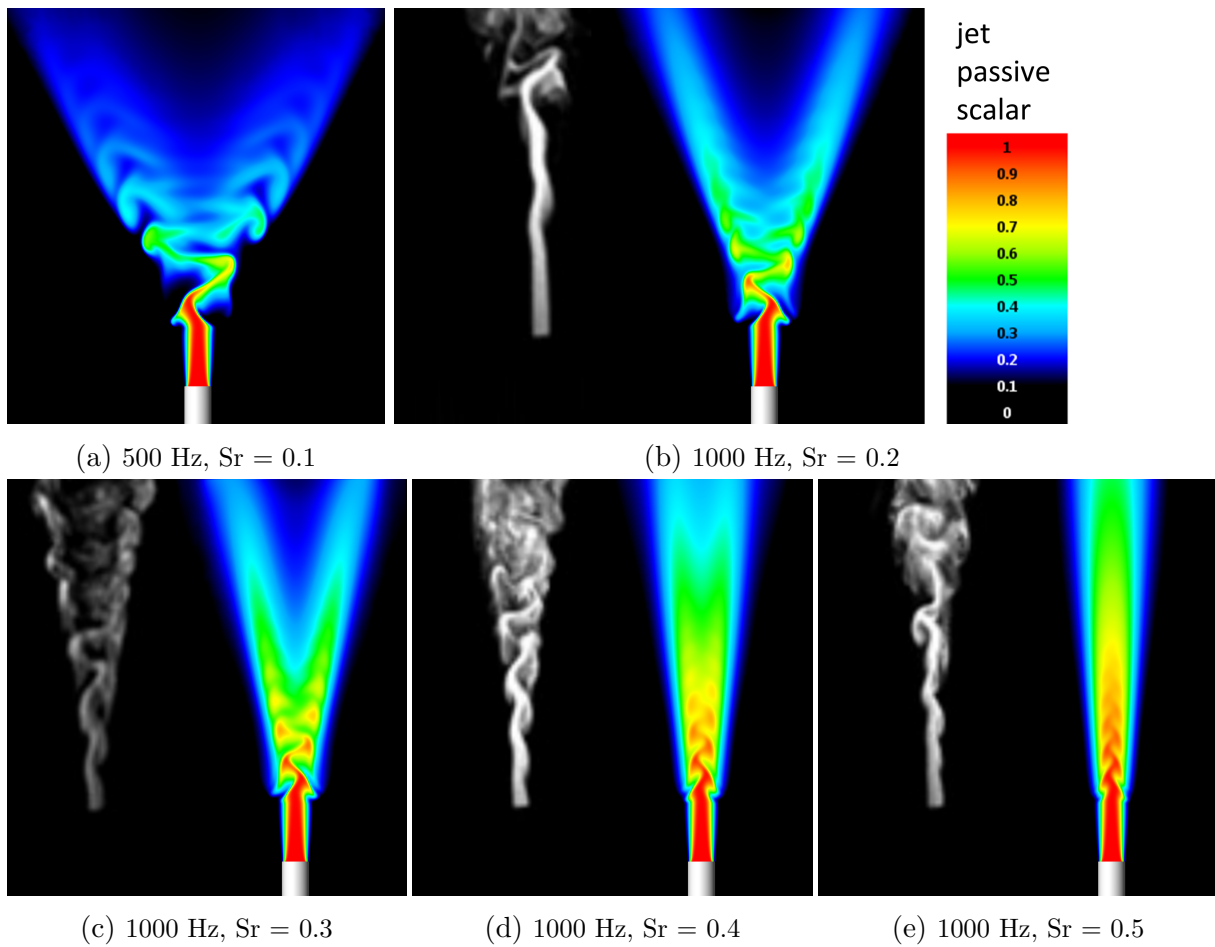


Figure 4. Jet passive scalar distribution. For (a) no experimental data provided

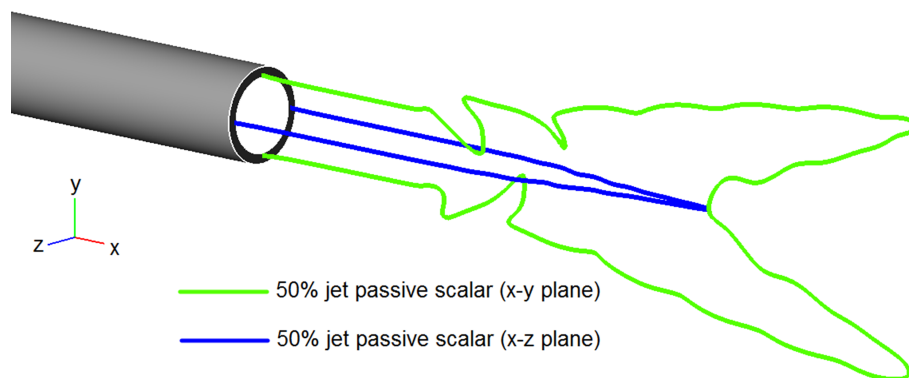


Figure 5. 3D jet visualization: 50% jet passive scalar contours in two planes

The streamlines in the jet and the co-current flow surrounding it are shown in Fig. 6. As follows from the image, the gas surrounding the jet is partially drawn into the area of the force action and the surrounding volume. Thus, mutual penetration of the jet and flow matter occurs, which enhances kinematic mixing.

The layers located far from the jet (at a distance of about 2 injector diameters) bend around the jet without mixing with it. Thus, the jet and the adjacent layers of the external flow form a domain within which the kinematic mixing of the layers occurs. However, the layers of this domain do not undergo kinematic mixing with the layers of the surrounding flow. At a distance

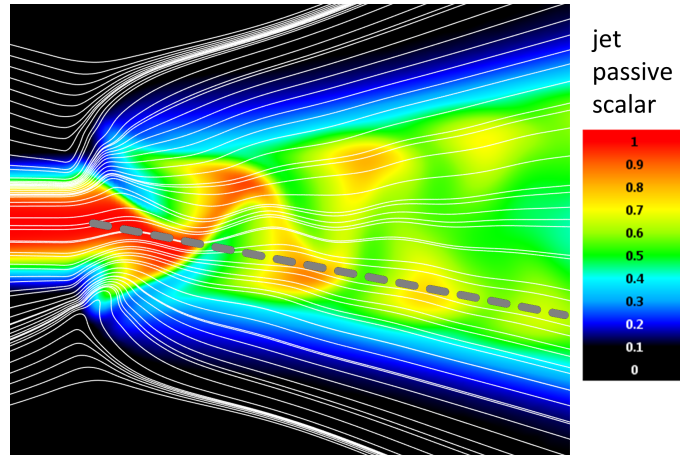
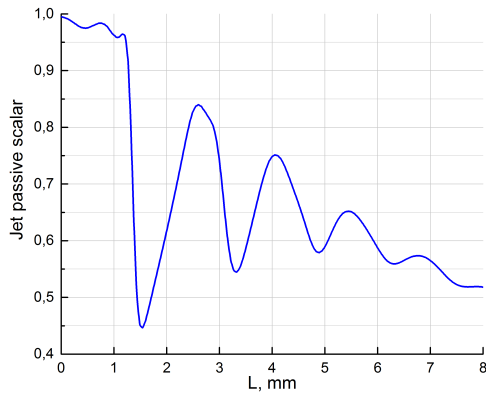


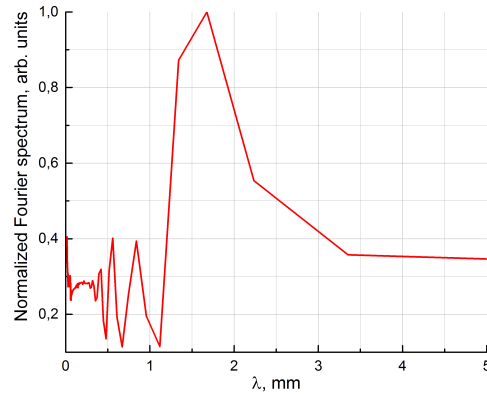
Figure 6. Streamlines in jet and surrounding stream and jet passive scalar

from the point of action of the force (about 5 jet diameters), the streamlines become almost straight. This means that with further propagation of the jet, mixing is caused mainly by molecular processes (diffusion).

The dashed line in Fig. 6 denotes a line directed along one of the two jet streams. The passive scalar profile along this line is shown in Fig. 7a. This profile illustrates how the jet substance mixes with the ambient air: both in the region of curved streamlines and in the region where the streamlines are straight. As follows from the figure, alternating portions of the jet and portions of external air gradually mix, causing the oscillations of the passive scalar to damp. At the same time, a general trend towards a decrease in the passive scalar is observed due to the divergence of the jet.



(a) Profile along a dotted line in Fig. 6



(b) Normalized Fourier transform of a part of the profile

Figure 7. Jet passive scalar distribution

On the right in Fig. 7b the Fourier spectrum obtained using the FFT is presented for the right part of the passive scalar graph (for the right stream). From this spectrum, one can determine the characteristic spatial period λ of the jet structure. In the work [18], a similar (with minor differences) analysis of the spatial frequency of disturbances was carried out based on the experiment for a frequency of 1000 Hz. The wavelength (1.5 ± 0.3) mm obtained in the simulation agrees well with the experiment.

The jet and the external force can be quantitatively compared by the momentum per unit of mass. For jet it is just the velocity $P_{jet} = U_0 = 5 \text{ m/s}$. The force momentum for the half period is $P_{force} = F/(\pi\rho fV) \sim 3 \text{ m/s}$, where $F = 5 \mu\text{N}$ is the amplitude of volumetric force, $V = 4.6 \cdot 10^{-10} \text{ m}^3$ is the volume of the region to which the force is applied, $\rho = 1.28 \text{ kg/m}^3$ is mass density, and $f \sim 1000 \text{ Hz}$ is frequency. These quantities, P_{jet} and P_{force} , are of the same order. This is in good agreement with the results of an experimental study of corona discharge [18] – the speed of the jet initiated by the corona is a few m/s with a width of 2 mm.

4. Results for 3D Simulation of Micro-Jet Excitation by Heat Source

Another possible mechanism for jet excitation is the pulse-periodic heating due to the discharge and the resulting pressure pulsations. To test the degree of influence of the thermal effect of the corona discharge on the jet using pulsed local heating, a case with a frequency of 1 kHz was selected. Volumetric heat release was activated in the area marked in red in Fig. 1. The periods of the presence and absence of heating alternated with a duty cycle of 50% (0.5 ms of heating and 0.5 ms of no heating). During the heating periods, the released power was 20 mW, while the maximum temperature rose to 320 degrees Celsius, which approximately corresponds to the average gas temperature in the corona discharge area. The pressure in the area near the pulsed heating site experienced jumps of up to 0.5 Pa at the moments of switching the heating on and off, but at other times the pressure changed insignificantly. Time dependencies of temperature and pressure in the area of discharge are presented in Fig. 8.

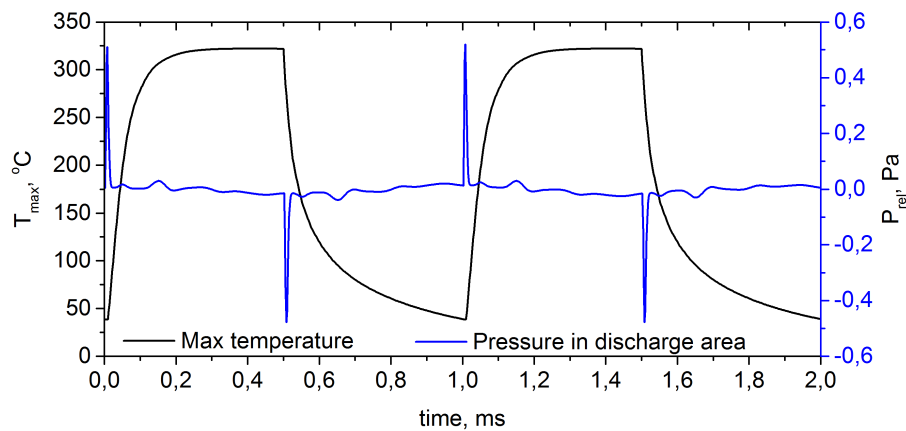


Figure 8. Time dependencies of temperature and pressure caused by pulse-periodic heat source operation at frequency 1000 Hz

The temperature distribution in the jet under the influence of pulse-periodic heating is shown in Fig. 9 on a logarithmic scale and in the form of contours against the background of the distribution of the passive scalar of the jet. Judging by the bends of the heated gas region, oscillations are observed in the jet, but their amplitude is insufficient to make the jet diverge (at least in the simulated section).

Figure 10 allows us to compare the pressure distribution in the jet in the cases of the action of a periodic volumetric force (a) and a periodic heat source (b). The pressure differences excited by local heating are an order of magnitude smaller than the pressure differences arising under the action of an external force.

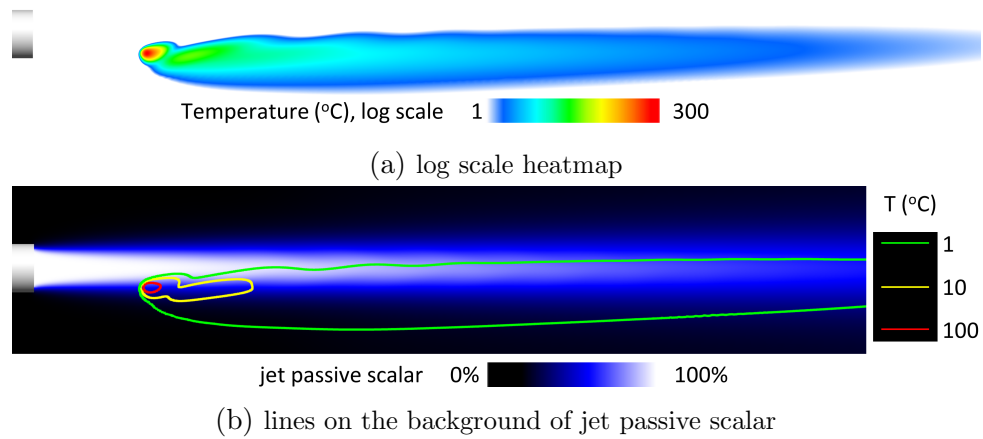


Figure 9. Distributions of temperature in case of pulsed heating

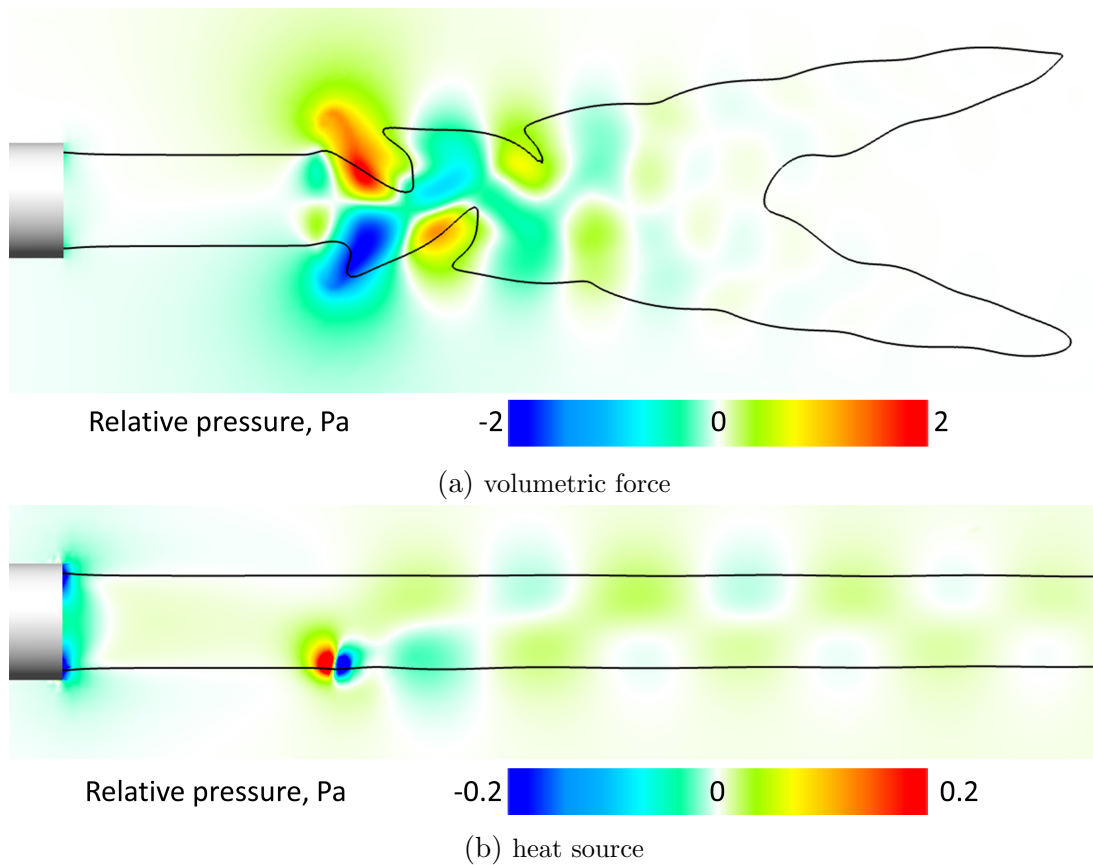


Figure 10. Pressure distribution in cases of jet excitation by volumetric force and heat source

The velocity distributions in the jet for the two indicated mechanisms of jet excitation are shown in Fig. 11. For the case of periodic volumetric force, the gas velocity drops rapidly: at a distance of about three jet diameters from the point of action, it no longer exceeds half the initial value. And in the case of periodic heat action, the jet retains its velocity longer, and the heat source introduces only a barely noticeable distortion into the velocity distribution.

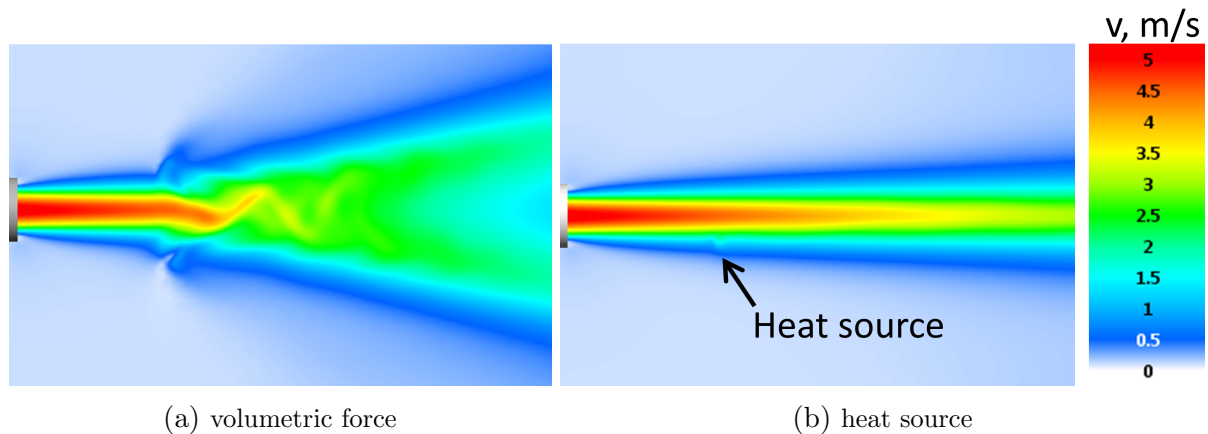


Figure 11. Velocity distribution in cases of jet excitation by volumetric force and heat source

Conclusion

The volumetric force and pulse-periodic heat source excitation of a round laminar air micro-jet at normal conditions were simulated using the FlowVision software package. The jet diameter was 1 mm, velocity had Poiseuille profile with the maximum of about 5 m/s. For this case, the effect of two mechanisms that could be responsible for the excitation of the jet affected by corona discharge was considered: a volumetric oscillating force with an amplitude of 5 μN and a pulse-periodic heat release with a power of 20 mW.

The numerical modeling shows that the volumetric force (ion wind) is the main mechanism responsible for the excitation of jet oscillations under the influence of a corona discharge. Another supposed mechanism of the discharge action – volumetric heat release – turned out to play no significant role in the effect on the jet.

For several values of the discharge voltage in the experiment from the article [18], the amplitude of the external sinusoidal force was selected, which in computer modeling leads to effects similar to those observed in the experiment when a corona discharge affects a laminar jet. The dependence of the jet shape on the frequency of the external force was investigated. It is shown that, depending on the frequency of the force, the following can occur in the jet:

- perturbations that do not significantly affect the shape of the jet, and partial mutual penetration of the outer layers of the jet and the adjacent layers of the surrounding air (2500 Hz, 2000 Hz) can occur;
- the jet may bifurcate, i.e., split into two streams (1500 Hz, 1000 Hz);
- the jet may break up into separate fragments (500 Hz).

The structure of the jet in case of bifurcation was considered in detail, the structure of the jet streams during bifurcation was described, the main mixing mechanisms and the place of their dominance were indicated. The obtained results of modeling when simulating a discharge using a volumetric force are in satisfactory agreement with the experimental results.

Acknowledgements

This work was performed within the State Assignment No. 075-00270-24-00 by the Ministry of Science and Higher Education of the Russian Federation.

This paper is distributed under the terms of the Creative Commons Attribution-Non Commercial 3.0 License which permits non-commercial use, reproduction and distribution of the work without further permission provided the original work is properly cited.

References

1. Reynolds, W.C., Parekh, D.E., Juvet, P.J.D., *et al.*: Bifurcating And Blooming Jets. Annual Review of Fluid Mechanics 35(1), 295–315 (2003). <https://doi.org/10.1146/annurev.fluid.35.101101.161128>
2. Perumal, A.K., Zhou, Y.: Axisymmetric jet manipulation using multiple unsteady minijets. Physics of Fluids 33(6), 065124 (2021). <https://doi.org/10.1063/5.0052275>
3. Gau, C., Shen, C.H., Wang, Z.B.: Peculiar phenomenon of micro-free-jet flow. Physics of Fluids 21(9), 092001 (2009). <https://doi.org/10.1063/1.3224012>
4. Yamani, S., Keshavarz, B., Raj, Y., *et al.*: Spectral Universality of Elastoinertial Turbulence. Physical Review Letters 127(7), 074501 (2021). <https://doi.org/10.1103/PhysRevLett.127.074501>
5. Yoshida, H., Koda, M., Ooishi, Y., *et al.*: Super-Mixing Combustion Enhanced by Resonance between Micro-Shear Layer and Acoustic Excitation. Int J Heat Fluid Flow 22(3), 372–379 (2001). [https://doi.org/10.1016/S0142-727X\(01\)00103-5](https://doi.org/10.1016/S0142-727X(01)00103-5)
6. Krivokorytov, M.S., Golub, V.V., Volodin, V.V.: The effect of acoustic oscillations on diffusion combustion of methane. Technical Physics Letters 38(5), 478–480 (2012). <https://doi.org/10.1134/S1063785012050240>
7. Kozlov, G.V., Grek, G.R., Sorokin, A.M., *et al.*: Influence of initial conditions at the nozzle exit on the structure of round jet. Thermophysics and Aeromechanics 15(1), 55 (2008). <https://doi.org/10.1134/S0869864308010046>
8. Kozlov, V.V., Grek, G.R., Litvinenko, Y.A., *et al.*: Subsonic Round and Plane Jets in the Transversal Acoustic Field. Siberian Journal of Physics 5(2), 28–42 (2010). <https://doi.org/10.54362/1818-7919-2010-5-2-28-42>
9. Krivokorytov, M.S., Golub, V.V., Moralev, I.A.: The evolution of instabilities in gas microjets under acoustic action. Technical Physics Letters 39(9), 814–817 (2013). <https://doi.org/10.1134/S1063785013090186>
10. Kozlov, V.V., Grek, G.R., Dovgal, A.V., *et al.*: Stability of Subsonic Jet Flows. Journal of Flow Control, Measurement & Visualization 01(03), 94–101 (2013). <https://doi.org/10.4236/jfcmv.2013.13012>
11. Kozlov, V.V., Grek, G.R., Korobeinichev, O.P., *et al.*: Combustion of hydrogen in round and plane microjets in transverse acoustic field at small Reynolds numbers as compared to propane combustion in the same conditions (Part I). International Journal of Hydrogen Energy 41(44), 20231–20239 (2016). <https://doi.org/10.1016/j.ijhydene.2016.07.276>
12. Oh, J., Heo, P., Yoon, Y.: Acoustic Excitation Effect on NOx Reduction and Flame Stability in a Lifted Non-Premixed Turbulent Hydrogen Jet with Coaxial Air. International Journal of Hydrogen Energy 34(18), 7851–7861 (2009). <https://doi.org/10.1016/j.ijhydene.2009.07.050>
13. Reumschüssel, J.M., Li, Y., Nedden, P.M., *et al.*: Experimental jet control with Bayesian optimization and persistent data topology. Physics of Fluids 36(9), 095164 (2024). <https://doi.org/10.1063/5.0217519>

14. Nedden, P.M., Nissen, T., Reumschüssel, J.M., *et al.*: Surrogate-based modeling for investigating and controlling the response of an axisymmetric jet to harmonic forcing. AIAA SCITECH 2024 Forum. <https://doi.org/10.2514/6.2024-0462>
15. Firsov, A., Savelkin, K.V., Yarantsev, D.A., *et al.*: Plasma-enhanced mixing and flameholding in supersonic flow. *Philos. Trans. R. Soc. A* 373(2048), 20140337 (2015). <https://doi.org/10.1098/rsta.2014.0337>
16. Dolgov, E.V., Kolosov, N.S., Firsov, A.A.: The study of the discharge influence on mixing of gaseous fuel jet with the supersonic air flow. *Computer Research and Modeling* 11(5), 849–860 (2019). <https://doi.org/10.20537/2076-7633-2019-11-5-849-860>
17. Volkov, L.S., Firsov, A.A.: Modeling the influence of repetitively pulsed heating on the formation of perturbations at the boundary of a transverse jet in a supersonic crossflow. *Computer Research and Modeling* 15(4), 845–860 (2023). <https://doi.org/10.20537/2076-7633-2023-15-4-845-860>
18. Yarantsev, D.A., Moralev, I.A.: Forcing microjet instabilities by corona discharge. *Vestnik Obedinennogo Instituta Vysokih Temperatur* 12, 4–8 (2023). (in Russian) <https://doi.org/10.33849/2023401>
19. Shevchenko, A.K., Yakovenko, S.N.: Simulation of Instability Development in a Plane Submerged Jet at Low Reynolds Numbers. *Siberian Journal of Physics* 13(4), 35–45 (2018). <https://doi.org/10.25205/2541-9447-2018-13-4-35-45>
20. Eri, Q., Ding, W., Kong, D., *et al.*: Numerical Investigation of Jet Control Using Two Pulsed Jets under Different Amplitudes. *Energies* 15(2), 640 (2022). <https://doi.org/10.3390/en15020640>
21. Firsov, A.A.: 2D Simulation of Micro-Jet Excitation by Heat Source. *Supercomputing Frontiers and Innovations* 10(4), 12–20 (2023). <https://doi.org/10.14529/jsfi230402>
22. Aksenov, A.A.: FlowVision: Industrial computational fluid dynamics. *Computer Research and Modeling* 9(1), 5–20 (2017). <https://doi.org/10.20537/2076-7633-2017-9-5-20>
23. Aksenov, A.A., Zhlukto, S.V., Kashirin, V.S., *et al.*: Three-dimensional Numerical Model of Kerosene Evaporation in Gas Turbine Combustors. *Supercomputing Frontiers and Innovations* 10(4), 27–45 (2024). <https://doi.org/10.14529/jsfi230404>
24. Moralev, I., Bityurin V., Firsov A., *et al.*: Localized micro-discharges group dielectric barrier discharge vortex generators: Disturbances source for active transition control. *Proceedings of the Institution of Mechanical Engineers, Part G: Journal of Aerospace Engineering* 234(1) (2020). <https://doi.org/10.1177/0954410018796988>
25. Moreau, E., Audier, P., Benard, N.: Ionic wind produced by positive and negative corona discharges in air. *Journal of Electrostatics* 93, 85–96 (2018). <https://doi.org/10.1016/j.elstat.2018.03.009>